Development 135, 2695-2705 (2008) doi:10.1242/dev.025981

Dynamic Fgf signaling couples morphogenesis and migration in the zebrafish lateral line primordium

Virginie Lecaudey[1,*], Gulcin Cakan-Akdogan[1,*], William H. J. Norton[2] and Darren Gilmour[1,†]

The collective migration of cells in the form of cohesive tissues is a hallmark of both morphogenesis and repair. The extrinsic cues that direct these complex migrations usually act by regulating the dynamics of a specific subset of cells, those at the leading edge. Given that normally the function of tissue migration is to lay down multicellular structures, such as branched epithelial networks or sensory organs, it is surprising how little is known about the mechanisms that organize cells behind the leading edge. Cells of the zebrafish lateral line primordium switch from mesenchyme-like leader cells to epithelial rosettes that develop into mechanosensory organs. Here, we show that this transition is regulated by an Fgf signaling circuit that is active within the migrating primordium. Point sources of Fgf ligand drive surrounding cells towards a 'non-leader' fate by increasing their epithelial character, a prerequisite for rosette formation. We demonstrate that the dynamic expression of Fgf ligands determines the spatiotemporal pattern of epithelialization underlying sensory organ formation in the lateral line. Furthermore, this work uncovers a surprising link between internal tissue organization and collective migration.

KEY WORDS: Lateral line primordium, Zebrafish, Collective migration, Fgf, Rosette morphogenesis

INTRODUCTION

The directed migration of epithelial tissues can be considered to be the driving force of organogenesis (Friedl et al., 2004; Lecaudey and Gilmour, 2006). A common feature of migrating epithelia is that cells at the so-called leading edge adopt many features that are more typical of mesenchyme, including a loss of apicobasal polarity, reduced expression of epithelial markers, such as tight junction proteins, and increased numbers of dynamic filopodia. This change in cell state at leading regions has been termed a 'pseudo' epithelial-mesenchymal transition (PEMT), to take into account the fact that these cells remain in contact (Pastor-Pareja et al., 2004). This is a crucial step in epithelial morphogenesis, as these leading edge cells, in many contexts, are responsible for the detection of extrinsic cues and tissue guidance. Thus, one major aim has been to identify the signaling pathways that select and differentiate the leading cells from the rest of the group (Martin-Blanco and Knust, 2001). Key regulators of this decision include the c-Jun N-terminal kinases (JNKs) and other members of the family of mitogen-activated protein kinases (MAPKs), which are known to be required for the advancement of the leading edge of epithelia in a number of morphogenetic contexts (Xia and Karin, 2004). As MAPKs act as signaling hubs downstream of a number of cell surface receptors, the cellular responses that they elicit are highly dependent on extracellular signals.

One large class of extracellular signaling molecules that can act through MAPKs is the fibroblast growth factors (Fgfs). Fgfs regulate many different types of developmental processes (Affolter and Weijer, 2005; Thisse and Thisse, 2005). For example, Fgf signaling has been shown to promote the migration of mesodermal cells during gastrulation in both invertebrates and vertebrates (Ciruna and Rossant, 2001; Gryzik and Muller, 2004; Yang et al., 2002). During the development of the *Drosophila* respiratory system, polarized epithelial sacs produce dynamic membrane projections characteristic of 'leader' cells in response to nearby patches of the Fgf-ligand *branchless* (Sutherland et al., 1996; Cabernard and Affolter, 2005; Ribeiro et al., 2002). Here, Fgf acts as both a chemoattractant to determine the direction in which branches migrate and as a morphogen to select leader 'tip' cells from an equivalent group of epithelial cells, with this role going to the cell with highest levels of Fgf receptor activation (Ghabrial and Krasnow, 2006). How cells become arranged and organized behind the leading edge, however, is less understood.

The zebrafish lateral line primordium is a migrating epithelial placode whose function is to deposit a series of mechanosensory hair cell organ progenitors, termed proneuromasts, along a stripe of the chemokine Sdf1a (Cxcl12a – Zebrafish Information Network) that runs along each flank of the embryo (Ghysen and Dambly-Chaudiere, 2007). Interestingly, these organ progenitors, rather than being preassembled, form repeatedly during migration as multicellular rosette structures that appear behind the leading edge. Here, we exploit this interesting feature of lateral line morphogenesis to address how tissues become organized during migration, a poorly understood subject of general importance. Through the use of mutants and a reversible small-molecule inhibitor, we show that the activity of two Fgf ligands, Fgf3 and Fgf10, is required redundantly for both internal organization and tissue migration. By performing time-lapse imaging on embryos in which Fgf signaling is acutely inhibited or hyperactivated, we demonstrate that, surprisingly, the activation of Fgf signaling drives cells towards a 'non-leader' fate by increasing epithelial character, essentially the opposite effect from what has been described in other contexts. Finally, we show that the dynamic expression of point sources of Fgf ligands controls the spatiotemporal pattern of epithelialization underlying sensory organ formation in the lateral line.

[1]European Molecular Biology Laboratory, Meyerhofstrasse 1, Heidelberg, Germany.
[2]Institute of Developmental Genetics, GSF-Research Center for Environment and Health, Ingolstaedter Landstrasse 1, Munich, Germany.

*These authors contributed equally to this work
†Author for correspondence (e-mail: gilmour@embl.de)

Accepted 19 June 2008

MATERIALS AND METHODS

Fish stocks

Zebrafish (*Danio rerio*) were raised and staged as previously described (Westerfield, 1994; Kimmel et al., 1995). The following mutant strains were used: *fgf3/limabsent* (*lia*^{t24149}) (Herzog et al., 2004); *fgf10/daedalus* (*dae*^{tbvbo}) (Norton et al., 2005), *cxcr4b/odyseus* (*ody*^{JI049}). The *cldnb:gfp* transgenic line (Haas and Gilmour, 2006) and the *hsp70:dn-fgfr1* transgenic line were described previously (Lee et al., 2005). The *hsp70:fgf3-myc* (*hsp70:fgf3*) transgenic line was generated by placing full-length *fgf3-myc* (Maves et al., 2002) under the control of the zebrafish *hsp70* promoter (Halloran et al., 2000), using the Tol2 Kit (Kwan et al., 2007).

Whole-mount in situ hybridization, immunohistochemistry and hair cell labeling

In situ hybridizations (ISH) and immunofluorescence (IF) stainings were performed according to standard procedures. The *atoh1a*, *fgfr3* and *fgfr4* cDNA probes were cloned by RT-PCR. Primers used were as follows:

atoh1a-F, 5′-TCCGTCCCTGTATCCATAGC-3′;
atoh1a-R, 5′-GTTGAATGTTCCGTCCTCGT-3′;
fgfr3-F, 5′-CGGCACGAGCTTTCACACAG-3′;
fgfr3-R, 5′-AAACCCTAAAGCTCCCTGTTTTT-3′;
fgfr4-F, 5′-TATAATGATGCTTGGCACTATGAAA-3′; and
fgfr4-R, 5′-TGGGGAGATCTACTTGTACTCATTC-3′.

fgf10 (Ng et al., 2002), *fgfr1*, *fgfr2* and *pea3* (Roehl and Nusslein-Volhard, 2001) RNA probes were kind gifts from Carl Neumann. For IF, the following antibodies were used: rabbit aPKC (1/100; Santa Cruz), mouse ZO1 (1/200; Zymed), mouse acetylated-tubulin (1/1000; Sigma), rabbit GFP (1/500; Torrey Pines Biolabs) and mouse GFP (1/500; JL8, Clontech). For labelling the hair cells, 2- to 3-dpf embryos were incubated in FM4-64 (10 mg/ml; Molecular Probes) in embryo medium (E3) for 2 minutes and rinsed in fresh E3.

Morpholino injection

The morpholino targeting *atoh1a* (MoAtoh1a, 5′-ATCCATTCTGT-TGGTTTGTGCTTTT-3′; Gene-Tools, Oregon, USA) was described previously (Millimaki et al., 2007) and was injected at a concentration of 0.05 mM.

Heat-shock, SU5402 and DAPT treatments

hsp70:dn-fgfr1 and *hsp70:fgf3* embryos (30 hpf) were heat-shocked for 20 minutes at 37°C. For SU5402 treatments, 24-hpf *cldnb:gfp* embryos were dechorionated and incubated for 6 hours in 5 to 10 μM SU5402 in E3 (Calbiochem #572630). Control embryos were treated with E3 containing the same amount of DMSO. For time-lapse imaging during drug treatment, pretreated embryos were mounted with agarose and E3 each containing 60 μM SU5402. For washout experiments, embryos treated with SU5402 were washed in E3 containing 0.5% DMSO for 2 hours and mounted for imaging. For DAPT treatment *cldnb:gfp* embryos at 20ss were dechorionated and incubated in 100 μM DAPT in E3 for 10 hours.

Electron microscopy

Electron microscopy was performed as previously described (Pouthas et al., 2008).

Mosaic analysis

Mosaic embryos were generated by transplantation as described previously (Haas and Gilmour, 2006).

Imaging

Embryos were anesthetized in 0.01% Tricane and mounted on glass-bottom petri dishes (Mattek) in 1% low melting point agarose. Time-lapse imaging was performed on Perkin Elmer Spinning Disc (ERS, RS, LCI) and Olympus Fluoview 1000 confocal microscopes using 10×/NA0.3, 20×/NA0.75, 40× W/NA1.2 or 60× W/NA1.2 objectives. Usually, *z*-stacks were captured at 2-3 μm intervals and flattened by maximum projection in ImageJ.

Image processing

Image processing and measurements were performed with ImageJ 1.38 X. Overlays of visible ISH and GFP IF were obtained by inverting the NBT-BCIP image with ImageJ.

RESULTS

Fgf3 and Fgf10 are active within the migrating primordium

Previous work has shown that the Fgf-target gene *pea3* is expressed by the lateral line primordium as it migrates from head to tail along either flank of the embryo (Munchberg et al., 1999; Roehl and Nusslein-Volhard, 2001). We analyzed the expression of a number of Fgf ligands and receptors in order to determine which are responsible for *pea3* activation in this context. Of the four characterized Fgf receptors, only *fgfr1* is clearly expressed in the migrating primordium (Fig. 1A, data not shown). This approach also identified two Fgf ligands, *fgf3* and *fgf10*, as being candidates for mediating signaling in this context. Interestingly, both genes are expressed within the primordium, being upregulated in leading regions (Fig. 1B,C). In addition, expression of *fgf10* can be clearly seen in one or two cells at the centre of rosette-like proneuromasts (Fig. 1C, arrows), whereas *fgf3* cannot be detected (Fig. 1B). Interestingly, the combined expression of these genes is somewhat complementary to that of *fgfr1* and *pea3*. Receptor and target are downregulated at the leading edge and at the centre of rosettes, both of which are sites of increased ligand transcription (Fig. 1A,D, arrows).

We next tested whether the activity of these ligands can account for the *pea3* expression pattern, by crossing the previously identified mutants *limabsent* (*lia*) and *daedalus* (*dae*), which encode mutations in *fgf3* (Herzog et al., 2004) and *fgf10* (Norton et al., 2005), respectively, to our previously described lateral line reporter, *cldnb:gfp* (Haas and Gilmour, 2006). Although the expression of *pea3* in the respective mutants is indistinguishable from wild type (wt; not shown), it is entirely absent from the migrating primordium of *fgf3;fgf10* double mutant embryos. Other embryonic expression domains, such as the somite borders and the midbrain-hindbrain boundary, however, remain unchanged (Fig. 1E-H). By comparison, embryos treated with the Fgf receptor inhibitor SU5402 for five hours show a complete absence of *pea3* expression throughout the embryo (Fig. 1I, J). We conclude that Fgf3 and Fgf10 mediate Fgf signaling during lateral line primordium migration.

Fgf3 and Fgf10 are required for migration and subdivision of the lateral line

We next addressed the requirement for Fgf signaling in lateral line morphogenesis. Single mutants for *fgf3* and *fgf10* showed no detectable change in lateral line development (Fig. 2A-C), a result that is consistent with normal *pea3* expression within the primordium in these embryos. By contrast, *fgf3;fgf10* double mutant primordia showed a number of striking defects when compared with wild-type controls (Fig. 2A,D). The most obvious difference was that the speed of migration was strongly reduced, with the primordium having migrated less than half the distance of wild type by 42 hours post-fertilization (hpf) (n=18; Fig. 2A,D,E). Furthermore, there was a change in morphology: the migrating primordia adopted an extended conformation, becoming twice as long as wild-type siblings (Fig. 2F,G,J). Similarly, blocking Fgf signaling with the Fgfr inhibitor SU5402, or using a heat-shock inducible, dominant-negative form of Fgfr1 (Lee et al., 2005), blocked migration and caused extended tissue morphology (Fig. 2H-J).

Closer inspection of double mutant primordia revealed that the assembly of neuromast progenitors was also strongly affected. Whereas two to three rosette-like neuromast organs can be morphologically identified within wild-type primordia (Fig. 2F), no such organization was visible in double mutants between 28 and 36 hpf (Fig. 2G, see also Fig. S1 in the supplementary material). Developmental timecourses revealed that, at later stages, organ

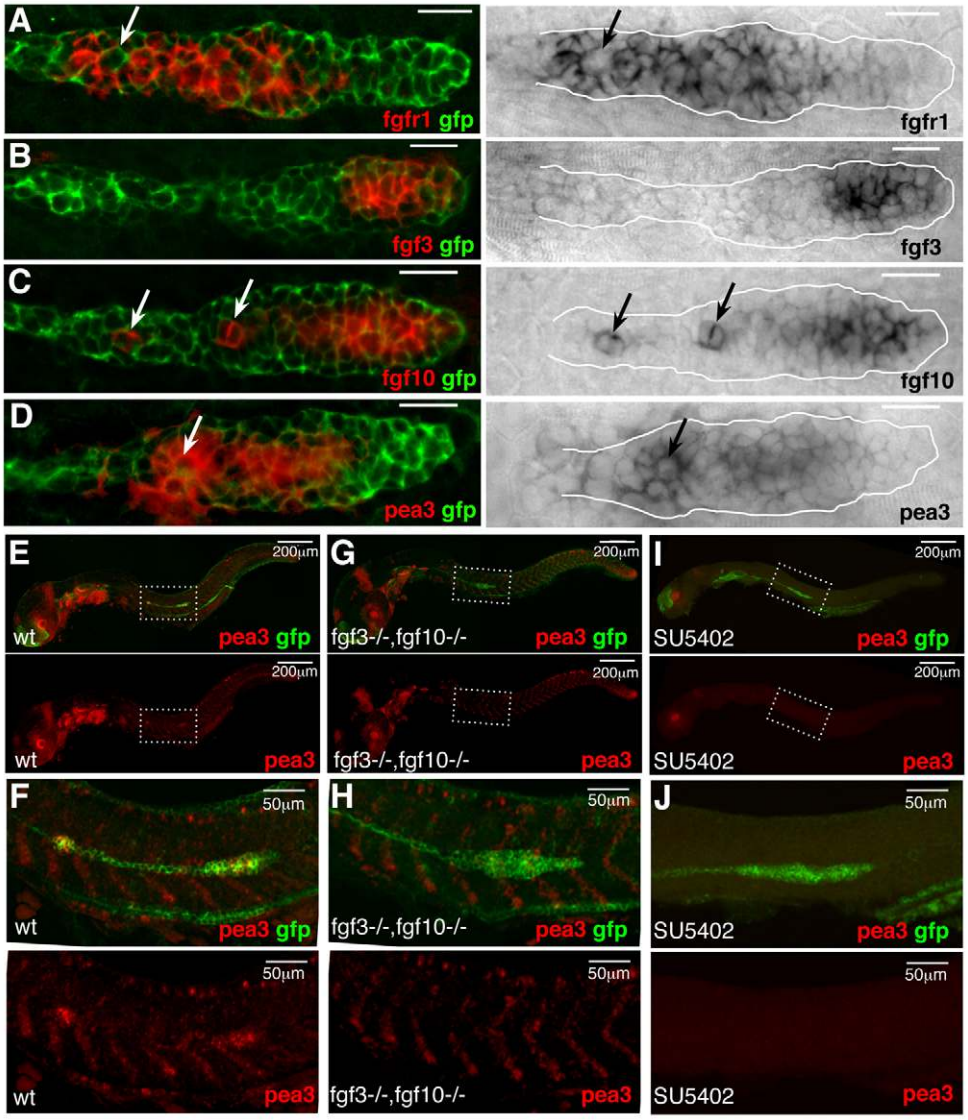

Fig. 1. FGF signaling is active in the migrating primordium. (**A-D**) Confocal images of the primordium in 36-hpf *cldnb:gfp* embryos labelled with a GFP antibody and indicated in situ hybridization probes. Right panels are transmission images of NBT-BCIP stainings, which were inverted and overlaid with GFP (left). Arrows point to *fgf10*-expressing cells (C), or to cells with reduced expression of *fgfr1* (A) or *pea3* (D). (**E-J**) Fluorescent images of 36-hpf *cldn:bgfp* wild-type (E,F), *fgf3;fgf10* double mutant (G,H) and SU5402-treated (I,J) embryos labelled with a *pea3* probe (red) and GFP (green). F,H and J are close-ups of the primordium in E,G and I (white dashed frames). Anterior is to the left. Scale bars: 20 μm (unless stated otherwise).

assembly defects are less pronounced, with 71% (n=14) of the double mutant primordia showing a normal number of rosettes. This recovery of rosettes could be due to the fact that the *fgf3* allele used has some residual activity (Herzog et al., 2004). Indeed, treating embryos with 5 μM SU5402 for 6 hours completely removes organ progenitors from the primordium (Fig. 2H). Given that only *fgf10* mRNA is detected in the centre of rosettes, the finding that rosette assembly was not affected in *fgf10* single mutants was somewhat surprising. However, expression analysis reveals that *fgf3* assumes an '*fgf10*-like' pattern in *fgf10* mutants, expanding posteriorly in the leading region and increasing at rosette centres (compare Fig. 2K with Fig. 1B).

On the basis of this analysis, it appears that Fgf signaling is required for several aspects of lateral line morphogenesis, including rosette assembly, tissue morphology and efficient migration. We therefore decided to address the relationship between these processes and the role of Fgf signaling in each.

Lateral line phenotype cannot be explained by a defect in neurogenesis

Given that Fgfs are known to be important for neuronal differentiation in a number of different contexts (Akai et al., 2005; Henrique et al., 1997; Millimaki et al., 2007; Nechiporuk et al., 2007), the lack of rosette assembly and aberrant migration in *fgf3;fgf10* double mutants could result from a disruption in the neurogenesis program that is initiated within the migrating primordium. Support for this suggestion comes from studies on the zebrafish ear, the organ most closely related to the lateral line primordium, where it has been shown that Fgf drives neuronal development through the activation of the proneural gene *atoh1a* (Millimaki et al., 2007). Furthermore, it has been shown that *atoh1a* is expressed in the migrating primordium in a progressively restricted manner, in a large patch at the front of the primordium that becomes focused to one or two cells at the centre of forming rosettes (Itoh and Chitnis, 2001). This expression pattern, which is very similar to that of *fgf10*, has been proposed to become restricted by lateral inhibition (Itoh and Chitnis, 2001) and is required for the differentiation of hair cells (Sarrazin et al., 2006). Therefore, in order to test whether Fgf controls rosette formation via the activation of *atoh1a*, we analyzed the consequences of knocking down *atoh1a* on rosette assembly. Injection of an *atoh1a*-specific morpholino (Millimaki et al., 2007) led to a significant broadening of its own expression domain (Fig. 3A,B), as could be expected from a loss of lateral inhibition. Moreover, staining these morphant embryos with markers of hair cell differentiation, such as FM4-64 and anti-

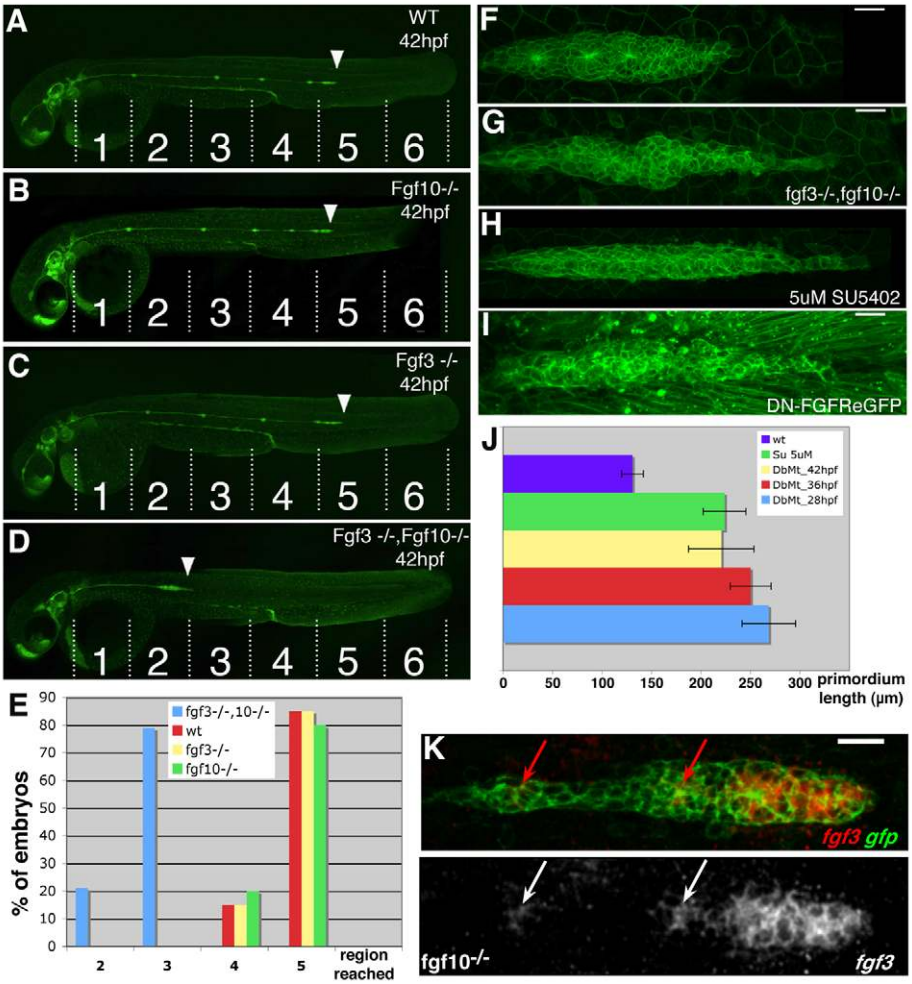

Fig. 2. FGF signaling is required for the migration and subdivision of the primordium into rosettes. (**A-E**) Lateral line migration in wild-type (A), *fgf10* mutant (B), *fgf3* mutant (C) and *fgf3;fgf10* double mutant (D) *cldnb:gfp* embryos at 42 hpf, quantified in E (*n*=18 for each genotype). (**F-I**) Representative primordia of wild-type (F), *fgf3;fgf10* double mutant (G), SU5402-treated (H) and heat-shock induced *dn-fgfr1* (I) embryos showing the stretched shape and the lack of rosettes resulting from the loss of Fgf activity. (**J**) The primordium length in each context (9 wild-type, 17 SU5402-treated and 7 *fgf3;fgf10* double mutant primordia were measured). (**K**) *fgf3* expression is expanded in *fgf10* mutants. Arrows point to the ectopic dots of *fgf3* expression in the center of rosettes. Anterior is to the left. Scale bar: 20 μm.

acetylated tubulin, revealed the expected loss of hair cells (Fig. 3G-J), confirming the efficacy of the morpholino. Beside the absence of hair cells, *atoh1a* morphant neuromasts were indistinguishable in number and morphology from wild type (Fig. 3E-J). Furthermore, imaging these embryos during earlier stages reveals that rosette assembly and neuromast deposition proceeded entirely normally in *atoh1a* morphants (Fig. 3C,D). We next blocked Notch activity completely by treating embryos with the γ-secretase inhibitor DAPT, a widely used antagonist of Notch signaling (Geling et al., 2002). Treatment with DAPT during lateral line migration resulted in an expansion of *atoh1a* expression in the primordium (not shown) and in deposited neuromasts (Fig. 3O,P), similar to that observed in *atoh1a* morphants, thus confirming drug efficacy. However, once again, this had no effect on the assembly of rosettes within the migrating primordium or on the pattern of deposited neuromasts (Fig. 3K-N). These findings show that rosette assembly is not dependent on neurogenesis, and that Notch-based lateral inhibition mechanisms do not play a crucial role in this process. Therefore, we conclude that the phenotype resulting from the loss of Fgf signaling is not a result of defective neurogenesis.

Primordium migration is uncoordinated in the absence of Fgf activity

The most striking phenotype resulting from a loss of Fgf signaling is the strongly reduced motility of the lateral line primordium, which, while remaining on the normal migration path, moves at less than half the speed and half the distance of wild type. Our previous work has shown that all cells of the lateral line primordium, with the exception of those at the trailing edge, migrate at the same velocity, resulting in a highly synchronous, smooth movement (Fig. 4A; see also Movie 1 in the supplementary material). However, tracking the migration of *fgf3;fgf10* double mutant primordia reveals a loss of coordination between the different regions of the primordium (Fig. 4B; see also Movie 2 in the supplementary material). Here, the primordium goes through cycles. First, the leading edge extends while cells behind remain stationary, causing the front part of the tissue to stretch. Then, the stretched leading edge halts, presumably when it reaches its limit, and cells behind inefficiently shunt forward (Fig. 4B,C). This results in an out-of-phase, 'inchworm' locomotion, where front and following regions move in an alternating manner (Fig. 4C). In order to better understand this migration defect at the single-cell level, we labeled single internal cells by transplantation. Treating these mosaic embryos with SU5402 leads to a similar uncoupling of movement of the leading and trailing regions, clearly visible in the 'zig-zag' pattern seen in kymographs generated from these time-lapse data (Fig. 4D,E). As for double mutant primordia, the tissue goes through several cycles of stretching and compression before coming to a halt (Fig. 4F; see Movie 3 in the supplementary material).

Proneuromast assembly is a prerequisite for normal primordium migration

In addition to being less coordinated, cells in central regions of the primordium do not become organized into proneuromasts in *fgf3;fgf10* double mutants. One possible explanation for this

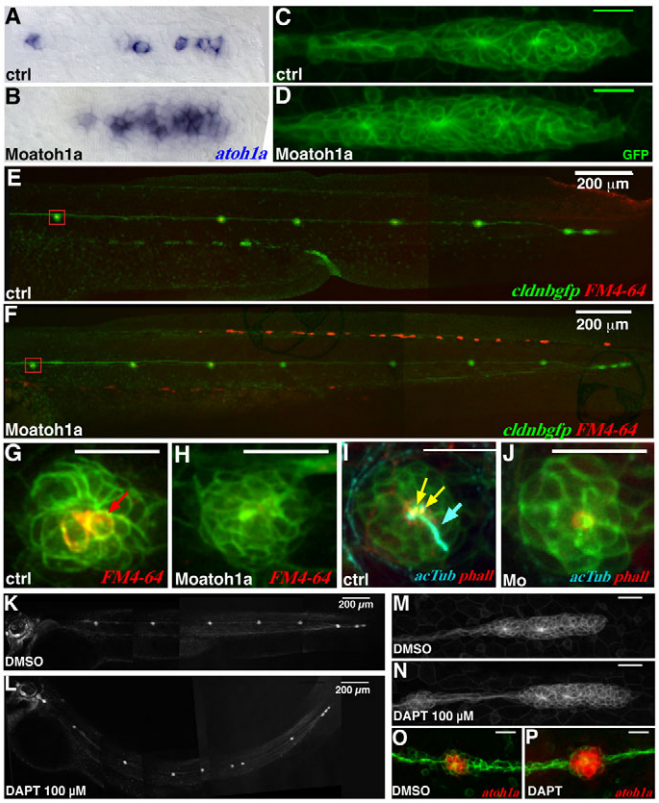

Fig. 3. Hair cell specification is not required for rosette assembly. (**A**,**B**) *atoh1a* expression is expanded in MoAtoh1a-injected embryos (B) compared with control embryos (A). (**C**,**D**) Live *cldnb:gfp* control (C) and MoAtoh1a-injected (D) embryos at 36 hpf. (**E**,**F**) The same embryos as in C,D imaged at 2.5 dpf, the number and position of neuromasts is within normal range. (**G**,**H**) Close-up view of a neuromast (red box in E,F), with hair cells labeled with FM4-64. Differentiated hair cells are present in wild type (red arrow) but absent in MoAtoh1a-injected embryos. (**I**,**J**) Loss of hair cells was confirmed by using an anti-acetylated tubulin antibody that labels the kinocilium (blue, blue arrow). (**K**,**L**) The primordium in embryos treated with 100 μm DAPT shows a normal pattern of neuromast deposition. (**M**,**N**) Primordia in DAPT and control embryos are indistinguishable. (**O**,**P**) The loss of restricted *atoh1a* expression in deposited neuromasts confirms the efficacy of DAPT treatment. Scale bars: 20 μm (unless otherwise stated).

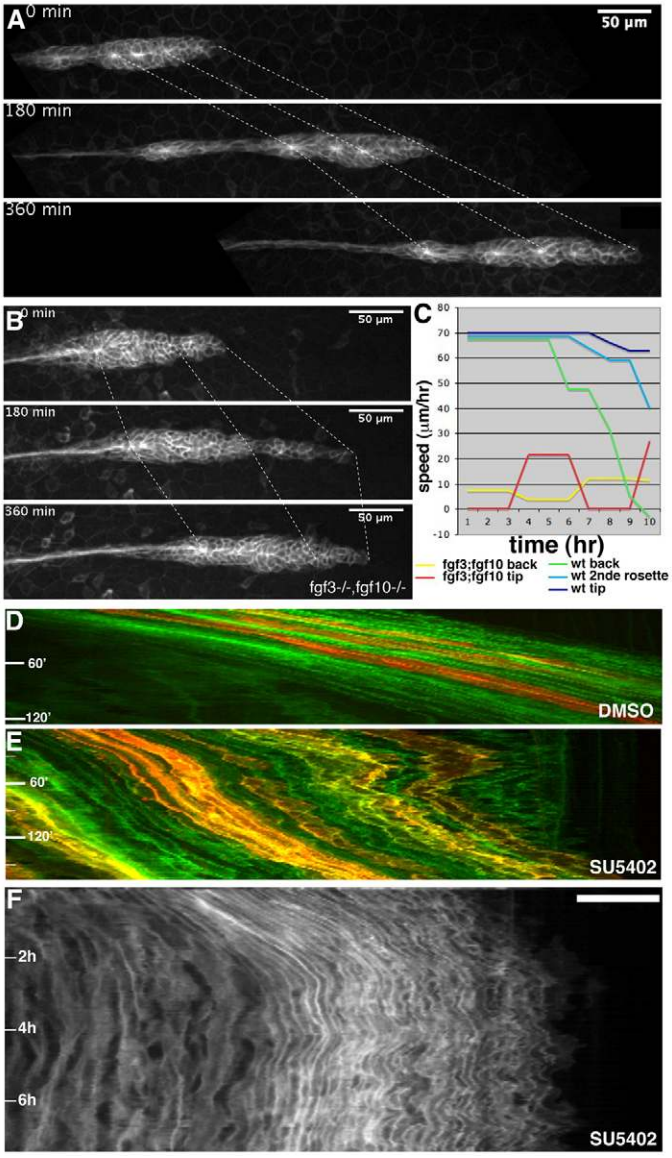

Fig. 4. The primordium migrates in an uncoordinated manner in the absence of FGF activity. (**A**) Images from a time-lapse movie of wild-type migration, velocity 69 μm/hour. (**B**) Images from a time-lapse movie of a *cldnb:gfp fgf3*$^{-/-}$*;fgf10*$^{-/-}$ embryo taken over 6 hours, showing the uncoordinated migration of the front and the back, average velocity 11 μm/hour. (**C**) Graph showing the speed of migration of tip (dark blue), the second rosette (blue) and the back (green) of the wild-type primordium, and of the tip (red) and the back (yellow) of the double mutant primordium, over a 10-hour period. (**D**) Kymograph of wild-type migration; all cells move at a similar speed, as indicated by the parallel lines of the kymograph. (**E**) Kymograph of a 3-hour movie of an SU5402-treated mosaic wt primordium showing the uncoordinated migration of cells within the primordium. (**F**) Kymograph of an 8-hour movie of a SU5402-treated wt primordium showing the back and forth movement of the primordium before it stops.

phenotype is that this repeated stretching of the migrating primordium prevents the cells from becoming organized. Alternatively, given that the 'raison d'être' of the lateral line primordium is to generate neuromasts, an inability of cells to assemble into organ progenitors could lead to a migration arrest through the activation of an unknown checkpoint. In order to determine which is the primary defect, migration or rosette assembly, we tested whether blocking stretching could rescue the rosette-loss phenotype observed after Fgf inhibition. This was achieved by treating *cxcr4b* mutant primordia, which are unable to detect and extend along the stripe of the Sdf1a guidance cue (David et al., 2002; Haas and Gilmour, 2006; Li et al., 2004), with SU5402. Blocking Fgf in stationary *cxcr4b* mutant primordia also led to the 'melting' of formed rosettes, thus excluding the possibility that the loss of organ assembly is a consequence of aberrant migration (Fig. 5A,B). Further support for the idea that loss of rosette assembly is the primary defect resulting from loss of Fgf signaling came from examining the temporal relationship between rosette assembly/disassembly and changes in primordium migration. Time-lapse analyses performed on the primordia of SU5402-treated embryos clearly demonstrate that rosettes melt before any detectable effect on migration (Fig. 5C,D; see Movie 4 in the supplementary

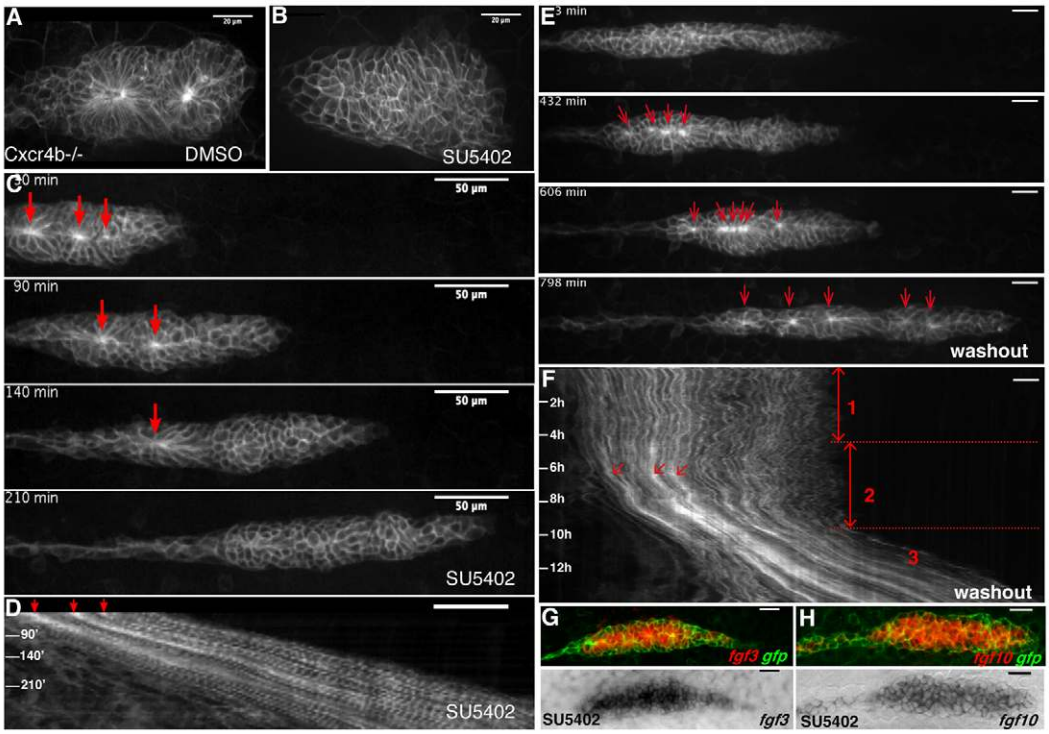

Fig. 5. FGF is required for rosette assembly, a prerequisite for primordium migration. Primordia of *cxcr4b* mutant embryos treated with DMSO (**A**) or SU5402 (**B**), showing the complete disappearance of rosettes after blocking the FGF pathway for 6 hours. (**C**,**D**) Time-lapse analysis and corresponding kymograph showing the progressive melting of rosettes after treatment with 80 μM SU5402. The migration speed is normal (70 μm/hour) and remains constant during this phase. Scale bar: 50 μm. (**E**,**F**) Time-lapse analysis and corresponding kymograph of a washout experiment showing that five rosettes (red arrows in E,F) simultaneously reassemble before migration resumes. Three phases can be distinguished on the kymograph: (1) uncoordinated migration, (2) rosette reassembly, and (3) migration recovery. (**G**,**H**) Expression of Fgf ligands in *cldnb:gfp* embryos treated for 6 hours with SU5402. Lower panels are transmission images of NBT/BCIP stainings. *fgf3* (G) and *fgf10* (H) are strongly expressed throughout the primordium when Fgfr is blocked. Scale bars: 20 μm (unless stated otherwise).

material). Interestingly, proneuromasts differ in their sensitivity to chemical inhibition of Fgf signaling, becoming increasingly resistant as they mature within the primordium. Only after all proneuromasts have disassembled does the stretched primordium halt its migration (Fig. 4F).

As the SU5402 inhibitor binds to Fgf receptors in a reversible fashion, we were able to perform 'washout' experiments to address if and how these stretched, arrested primordia can return to their normal state. Several hours after SU5402 washout, rosettes can be observed to reassemble within these primordia in the complete absence of migration (arrows in Fig. 5E,F). Once rosettes are reformed, the primordium recommences its caudal migration at normal velocity (Fig. 5F; see Movie 5 in the supplementary material). We conclude that loss of Fgf signaling prevents the subdivision of the primordium into proneuromasts, which, in turn, leads to an arrest of migration.

Surprisingly, closer analysis of time-lapse movies capturing SU5402 washout indicates that rosettes reappear by de novo assembly. Both the position and the temporal sequence in which these rosettes reappear were unpredictable, suggesting that the initial pattern of *fgf10* foci is lost through blocking Fgf-receptor activity. Indeed, in SU5402-treated embryos and in *fgf3;fgf10* double mutants, the transcription of both *fgf3* and *fgf10* was strongly enhanced and expanded to fill the entire primordium (Fig. 5G,H; see also Fig. S2 in the supplementary material). This reveals the existence of a negative-feedback loop in which the activation of Fgfr restricts the expression of its own ligands. This finding may explain the mutually exclusive expression of ligand and receptor observed during normal development (Fig. 1A-D).

Fgf spots increase epithelialization within the migrating primordium

One important step towards understanding how Fgf drives rosette assembly is to define the cell-shape changes underlying this morphogenetic process. Transmission electron microscopy reveals that proneuromasts are radially organized assemblies of pear-shaped epithelial cells that display constricted apical surfaces (Fig. 6A,B). Higher magnification views of the rosette center highlighted the presence of the three types of cell-cell junctions, tight junctions, adherens junctions and desmosomes, arranged in the apicobasal order that is typical of epithelia (Fig. 6B). Furthermore, antibodies against the apical marker aPKC and the tight junction protein ZO-1 (Tjp1 – Zebrafish Information Network), a widely used marker of epithelia, showed highly specific labelling at the centre of rosettes, confirming these as foci of apical membrane material and intercellular adhesion junctions (Fig. 6C,D). Both markers were excluded from the less-organized leading region. These foci also show increased levels of phalloidin staining (Fig. 6E), most likely due to the presence of the actomyosin ring responsible for apical constriction. In order to capture this organ formation process as it happens, we performed time-lapse imaging of embryos mounted in a 'side-view' orientation that allows the visualization of basolateral

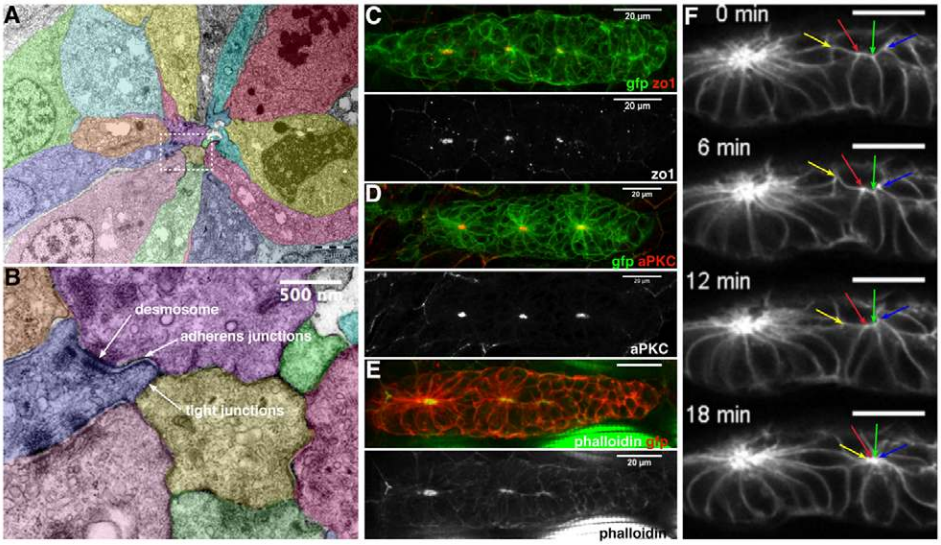

Fig. 6. Rosettes are radial clusters of apically constricted epithelial cells. (**A**) Electron micrographs of an apical section of a rosette; false-colouring highlights individual cells. (**B**) Close-up of the centre of the rosette, corresponding to the framed area in A. (**C-E**) Immunostaining using antibodies against GFP and ZO-1 (C), GFP and aPKC (D), and GFP plus phalloidin staining (E). Tight junction protein ZO1 and aPKC are only expressed at the center of each rosette; phalloidin-labeling reveals enriched actin at centre of rosette. (**F**) Time-lapse analysis of wild-type rosette formation reveals a coordinated constriction of the apical surfaces of several cells. Arrows point to the vertices of these cells as they coalesce. Scale bars: 20 μm (unless stated otherwise).

surfaces. By focusing on cells at the rear of the leading region, we could show that proneuromasts do indeed form through the simultaneous apical constriction of neighbouring cells (Fig. 6F; see Movie 6 in the supplementary material).

In *fgf3;fgf10* double mutants and SU5402-treated primordia, the epithelial tight junction protein ZO-1 was undetectable (Fig. 7A-C). Furthermore, viewing wild-type primordia side-on reveals that cells comprising rosettes are easily distinguished from the leading edge as a result of their heightened columnar morphology (Fig. 7D,F). By contrast, this distinction is lost in SU5402-treated embryos, as SU5402 treatment gives the primordium a 'flattened profile' (Fig. 7E,G). This lack of apicobasal polarization was confirmed by measuring the height:width ratio of individual cells, which is halved in SU5402-treated primordia when compared with rosette-forming regions in wild type (Fig. 7H). Time-lapse analysis of SU5402-washout embryos mounted side-on confirms that cells of the primordium adopt a heightened, columnar morphology before local apical constrictions become visible (see Fig. S3 and Movie 7 in the supplementary material). Finally, analyzing the morphology of individual cells behind the leading edge revealed a clear increase in dynamic filopodial projections in SU5402-treated primordia when compared with single cells in the same position in DMSO-treated primordia, a further indicator of increased mesenchyme-like characteristics (Fig. 7I-L; see Movies 8 and 9 in the supplementary material). Collectively, these data allow us to conclude that, during wild-type morphogenesis, cells behind the leading edge undergo a transition to become columnar epithelia before snapping together via apical constrictions to form rosettes. In the absence of Fgf signaling, this switch in cell state does not occur, cells maintain leading edge characteristics and are unable to form rosettes.

In order to further test this hypothesis, we generated a stable transgenic line expressing *fgf3* under the control of the *hsp70* promoter (Halloran et al., 2000). In situ hybridization with an *fgf3* probe revealed that this ligand was expressed at an extremely high level throughout the entire embryo 4 hours after heat-shock induction (Fig. 7M,N). Rosettes were lost after heat-shock-induced overexpression of *fgf3* (data not shown), supporting a model in which discrete spots are required to seed and maintain rosettes. However, by 9 hours after heat shock, *hsp70:fgf3* embryos showed a significantly increased number of rosettes per primordium, when compared with identically treated, non-transgenic siblings (Fig. 7O-Q). Interestingly, the size of the rosette-free leading region was strongly reduced or even absent in *hsp70:fgf3* embryos, as confirmed by measuring the distance from the centre of the first rosette to the tip (Fig. 7R). Therefore, the misexpression of Fgf ligands causes a shift in the composition of the primordium, such that there is an increase in epithelialization at the expense of the mesenchyme-like leading region.

DISCUSSION

Turning leaders into followers

During branching morphogenesis in *Drosophila*, increased levels of Fgf receptor activity are known to select 'leading' tip cells from 'following' branch cells (Ghabrial and Krasnow, 2006). Here, we show that Fgf signaling plays a complementary role during lateral line development, that is, it allows cells of the primordium to adopt a fate other than that of the leading edge. As cells pass from the leading to the organ-forming region, they become responsive to Fgf signaling and adopt a textbook, epithelial morphology, resulting in increased cell packing and order. At what level does Fgf act to drive this change in cell phenotype? Loss of Fgf signaling results in a number of deviations from normal cell shape and behaviour, including the loss of apical constrictions and coordinated migration, which could potentially explain the inability of the cells to become assembled into rosette-like proneuromasts. However, the length of time required to either induce the phenotype with SU5402, or reinstate normal morphology by SU5402-washout, is in the range of hours. Such a sluggish response would not be expected if Fgf signaling were to act specifically as an internal guidance cue or drive apical constriction through the direct activation of the actomyosin system. Furthermore, Fgf-deficient primordia show an absence of the tight junction protein ZO-1, which is unlikely to be due to a concentration effect but rather to reduced expression of this epithelial marker. Indeed, that Fgf signaling drives fate decisions in this context is already apparent from our finding that active signaling through Fgfr is required to restrict the pattern of transcription of *fgf3* and *fgf10* (discussed below). These and other findings suggest that patterned Fgf signaling leads to a switch in local cell state, such that cells increase their epithelial character. Although this does not exclude that Fgf signaling additionally

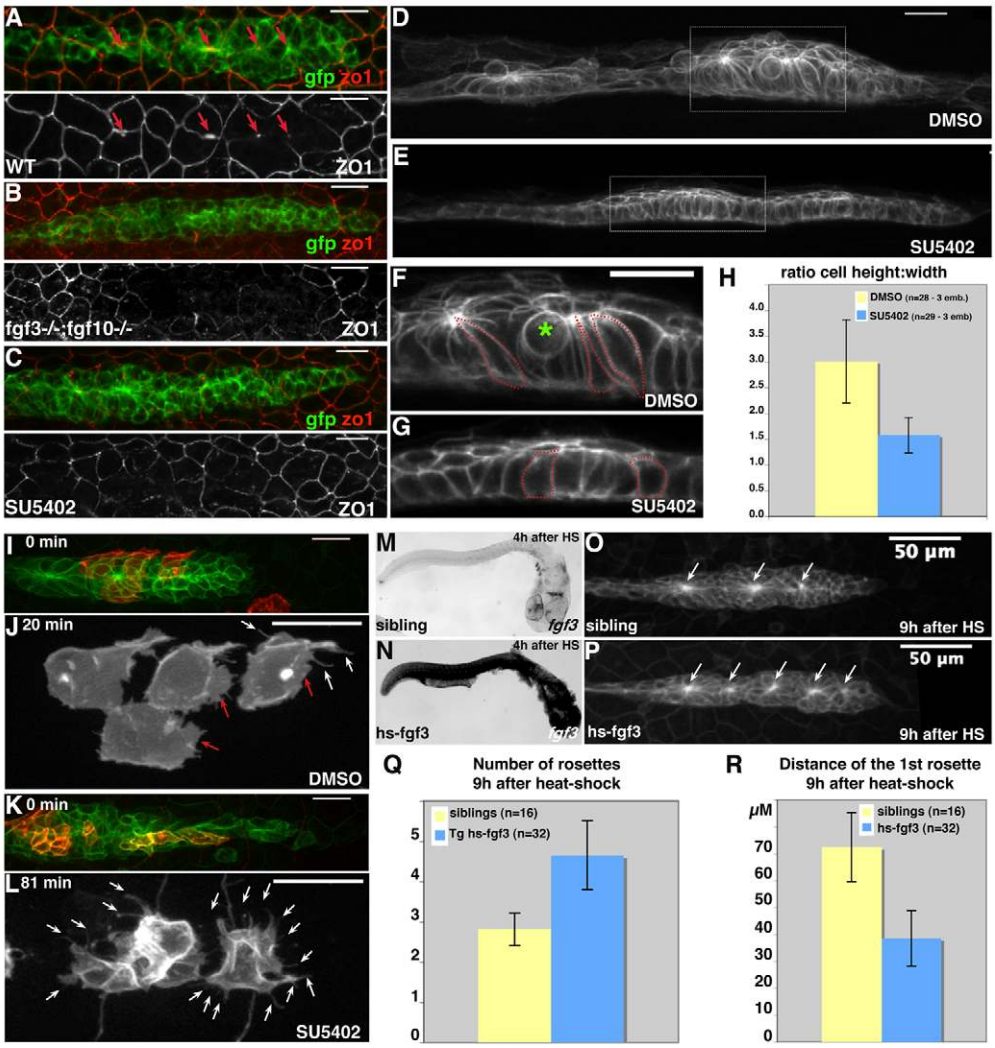

Fig. 7. FGF signaling nucleates rosette assembly via a radial epithelialization process. (**A-C**) Immunostainings with GFP and ZO-1 antibodies in wild type (A), *fgf3;fgf10* double mutants (B) and SU5402-treated embryos (C). Although ZO-1 is highly expressed in the centre of rosettes in wild-type primordia (arrows), it is completely absent from primordia lacking FGF activity. (**D-H**) Cells lacking FGF signaling are flatter and wider than control primordial cells. Confocal images show the primordium from the side in DMSO (D,F), and in SU5402 (E,G). F and G are close-up views of the boxed area in D and E; D and E are maximal projections, F and G are single *z*-planes. Red dashed lines outline single cell contour and the green star shows a rounded dividing cell (F,G). (H) Quantification of the cellular height:width ratio measured for 28 DMSO-treated (yellow) and 29 SU5402-treated (blue) cells from three different embryos in each case. This shows that cells deprived of FGF signaling have a rather cuboidal shape, whereas control cells have a columnar shape. (**I-L**) Confocal images of primordium showing single-cell behaviour in mosaic wild-type primordia exposed to DMSO (I,J) or to 5 µM SU5402 (K,L). Red and white arrows (J,L) point to lamellipodia and filopodia, respectively. (**M-R**) Global activation of *fgf3* expression under the control of a heat-shock promoter. (M,N) *fgf3* ISH 4 hours after heat shock of a sibling non-transgenic (M) and a *hsp70:fgf3* (N) embryo. (O,P) Live pictures of a sibling (O) and *hsp70:fgf3* (P) *cldnb:gfp* embryos 9 hours after heat shock. (Q,R) Quantification of the number of rosettes (Q) and the distance between the centre of the first rosette and the tip of the primordium (R) 9 hours after heat shock, showing that ectopic rosettes form in the leading region of the heat-shocked *hsp70:fgf3* primordium. Scale bars: 20 µm (unless stated otherwise).

regulates cell movement and apical constriction directly, we would imagine that the loss of these activities alone would be insufficient to explain the observed phenotype.

Dynamic changes in Fgf signaling control the spatiotemporal pattern of epithelialization within the primordium

The switch in cell state within the primordium can be considered to be a pseudo mesenchymal-epithelial transition (PMET). Therefore, we would predict that this process could be blocked by interfering with any one of a number of proteins required for epithelial morphogenesis, such as the general regulators of apicobasal polarity. However, our demonstration that this epithelialization process is controlled by the dynamic expression of specific Fgf ligands provides the first insight into the spatiotemporal regulation of lateral line organ formation. That this function is mediated by Fgf signaling was, to our knowledge, not at all predictable from previous work. On the contrary, elegant studies on chick somitogenesis have demonstrated that a gradient of Fgf signaling actually prevents the mesenchymal-epithelial transition that converts paraxial mesenchymal cells into epithelialized somites (Baker et al., 2006; Dubrulle et al., 2001; Dubrulle and Pourquie, 2004). As both

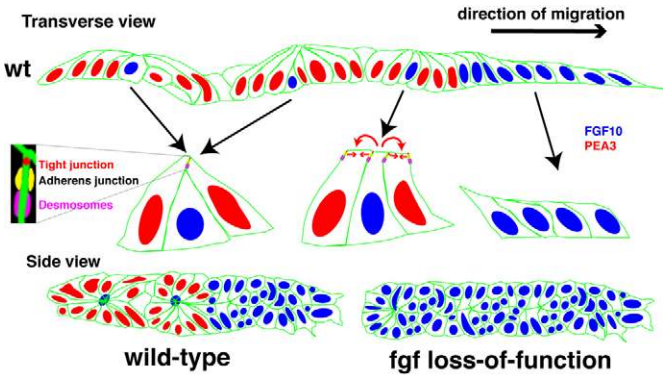

Fig. 8. Model of the FGF-driven radial epithelialization leading to rosette assembly. Blue nuclei correspond to cells expressing Fgf ligands. The red nuclei correspond to cells expressing *fgfr1* and *pea3*. In the leading region, cells have a mesenchymal-like characteristic. In the trailing region, Fgf-expressing cells retain mesenchymal fate (blue) and induce the epithelialization of their neighbors. These fully epithelial cells then 'close the gap' that represents the different cell in the middle by coordinated apical constriction and, as a consequence, form a rosette. In absence of FGF activity, all cells are equally mesenchymal-like and no rosette can form.

systems generate a series of repetitive epithelial packets from less-ordered mesenchymal cells, the similarities are striking, and it is therefore intriguing that Fgf signaling promotes EMT in one context but MET in another.

A crucial step towards understanding the periodicity of this system was to define how the dynamic pattern of *fgf10* dots that nucleate rosettes is generated. In situ hybridization revealed that *fgf10* is expressed in a broad patch at the front of the primordium that apparently becomes focused to one or two cells in organ-forming regions. This transcription pattern is highly reminiscent of that described for the proneural gene *atoh1a*, where focused expression is thought to be controlled by Notch-based lateral inhibition (Itoh and Chitnis, 2001). It was therefore surprising that perturbing Notch-based lateral inhibition, either by *atoh1a* knockdown or by treatment with the Notch antagonist DAPT, had no clear effect on rosette assembly or on the final pattern of neuromasts. This is consistent with the finding that *mindbomb* mutants have reduced Notch activity but a seemingly normal pattern of deposited neuromasts (Itoh and Chitnis, 2001). So how does *fgf10* expression get restricted to dots? Interestingly, *fgf10* and *fgfr1* show mutually exclusive expression during organ assembly, suggesting that *fgf10* expression may become restricted via a negative-feedback loop. Furthermore, the expression of both ligands expands throughout the entire primordium in *fgf3;fgf10* double mutants and SU5402-treated embryos, giving credence to the idea that Fgfr1 activity directly restricts Fgf ligand expression, possibly through a lateral inhibition-type mechanism. Interestingly, inactivating *fgf10* alone, through the use of *fgf10* mutants, leads to the formation of rosettes that are nucleated by dots of *fgf3*, a clear demonstration of the robustness of this pattern forming system.

A simple mechanism for generating rosettes within epithelia

In addition to determining the spatiotemporal pattern of epithelialization within the migrating primordium, Fgf signaling leads to the formation of rosette assemblies. The teleological reason for rosettes in this context is obvious, as these are the forerunners of neuromasts, a series of volcano-like organs that penetrate the skin to project mechansensory hairs cells into the surrounding water. Similar multicellular rosettes have recently been shown to arise in other epithelial tissues, suggesting that they could represent a common functional unit of epithelial morphogenesis (Blankenship et al., 2006; Brown et al., 2006; Wagstaff et al., 2008). They have been particularly well described in the context of *Drosophila* germband extension, where these transient rosettes directly participate in tissue elongation by forming and resolving in a directional manner that is influenced by embryonic anteroposterior patterning cues. Despite superficial similarities between these rosettes and those in the primordium, there are fundamental differences in their three-dimensional organization. The rosettes in the *Drosophila* blastoderm form when two rows of cells that are in contact with each other constrict their shared interface, that is, one side of their apical surface, with the resultant rosette resembling a pie where each slice is a cell (Blankenship et al., 2006; Zallen and Blankenship, 2008). The rosettes of the lateral line primordium, by contrast, assemble by bunching together cells whose entire apical surface is tightly constricted, with the resultant rosette resembling a garlic bulb where each clove is a cell. Another type of rosette that forms through the constriction of interfacial surfaces, rather than the entire apical surface, appears in the wake of the morphogenetic furrow that patterns the *Drosophila* retina. These arc-like rosettes, which are the forerunners of the ommatidia, are built around *atonal*-expressing R8 cells that 'recruit' surrounding cells in a stepwise fashion through the activation of the Egf-like ligand *spitz* (Brown et al., 2006). While the parallels with the lateral line system are clearly more obvious in this case, our demonstration that Notch signaling or Atoh1a is not required for rosette assembly suggests that there may be differences in the gene regulatory networks involved.

Collectively, our data lead us to propose the following model for rosette morphogenesis in the lateral line. An Fgf-based lateral inhibition-type system, like that suggested above, generates a single cell that expresses significantly higher levels of Fgf ligand and activates Fgfr1 in surrounding cells, as supported by upregulated *pea3* expression. As *fgf10* forms a point source, it induces the radial epithelialization of surrounding cells, which rise-up apicobasally and form tight junctions, as we have demonstrated. However, the central cell does not signal in an autocrine manner, as confirmed by the absence of *pea3* transcription, and is thus refractory to induction and maintains its mesenchyme-like state. This would result in a ring of heightened epithelial cells that has a flatter cell at its centre (Fig. 8). There are alternative scenarios for how this situation could be resolved to form a rosette. The most likely invokes the activation of a dedicated cell signaling system that leads to increased cohesion between the nucleating cell and the neighbouring epithelia, causing the latter to apically constrict and cover the former. As this apical constriction occurs over several cell diameters, the central cell may secrete a signal that ensures directionality, a function that could be fulfilled by *fgf10* itself. Alternatively, if the centre cell simply maintains its leading-edge characteristics, it may initiate rosette formation by triggering a response similar to wound healing in surrounding cells. This second scenario is somewhat simpler, as it generates rosettes by exploiting an intrinsic property of epithelium, which is to undergo coordinated apical constrictions whenever its integrity is disrupted (Jacinto and Martin, 2001; Martin and Parkhurst, 2004). Indeed, the rosettes that form within the lateral line are, at their core, more similar to those generated by wounding an epithelium than either of the developmental examples given above (Martin and Parkhurst, 2004). However, in the case of the lateral line, cells at the centre of the rosettes are not extruded and discarded

from the epithelium, as damaged cells are during wound healing, but are rather encapsulated through this apical constriction process. These are most likely the cells that give rise to sensory hair cell progenitors within a few hours of this morphogenetic event.

Tissue compartmentalization is required for efficient migration

One of the surprising findings of this work is that a defect in the internal organization of the primordium has such a strong detrimental effect on its migration. This finding is perhaps counterintuitive, as increasing the relative proportion of cells with mesenchyme-like, leading edge fate could be expected to improve migration efficiency rather than decrease it. Given the numerous examples in which Fgf ligands have been shown to act as chemoattractants during cell migration (Affolter and Weijer, 2005), one alternative explanation for this result is that Fgf3/Fgf10 act as diffusible guidance cues that regulate directionality within the migrating primordium. However, several findings presented here make it unlikely that this is the primary role of internal Fgf signaling during primordium migration. Not only does directional migration continue normally for several hours after blocking Fgf signaling with SU5402, but a change in rosette assembly always prefigures a change in migration behaviour. Furthermore, ubiquitous, high-level expression of *fgf3* does not lead to a rapid change in tissue migration behaviour or direction, which would be expected if it were to act as a chemoattractant. Rather, we propose that the primordium possesses an internal checkpoint that halts migration whenever there is a problem with rosette assembly. Of course, a mechanism that couples migration behaviour to organ assembly makes biological sense, as a migrating primordium that does not deposit organs is of little use. As with rosette assembly, this checkpoint could be mediated through the activation of a dedicated signaling system or it may exploit intrinsic mechanical properties of the tissue. Indeed, rosette formation may facilitate migration simply by virtue of the fact that it converts a large number of migrating mesenchyme-like cells into two or three packets that could be controlled as single units, thus reducing the complexity of the system. Answers to such questions will come from a deeper understanding of the respective mechanical properties of epithelial and mesenchyme-like domains within migrating tissues.

We are grateful to Petra Haas for contributions to early stages of this work, to Kota Miura for expert feedback on image analysis, to Andreea Gruia for animal care and to Andreas Kunze for help with generating transgenes using the Tol2 Kit, which was a generous gift from Chi-Bin Chien. We thank Nga Ly-Hartig and Claude Anthony for assistance with EM, and the Advanced Light Microscopy Facility at EMBL for imaging advice. We thank Eric Karsenti, Sebastian Streichan, Lars Hufnagel, Francesca Peri and the Gilmour lab for stimulating discussions, and Francesca Peri for critical reading of the manuscript. V.L. was supported by fellowships from EMBO and Marie Curie FP6.

Supplementary material

Supplementary material for this article is available at
http://dev.biologists.org/cgi/content/full/135/16/2695/DC1

References

Affolter, M. and Weijer, C. J. (2005). Signaling to cytoskeletal dynamics during chemotaxis. *Dev. Cell* **9**, 19-34.
Akai, J., Halley, P. A. and Storey, K. G. (2005). FGF-dependent Notch signaling maintains the spinal cord stem zone. *Genes Dev.* **19**, 2877-2887.
Baker, R. E., Schnell, S. and Maini, P. K. (2006). A clock and wavefront mechanism for somite formation. *Dev. Biol.* **293**,116-126.
Blankenship, J., Backovic, S., Sanny, J., Weitz, O. and Zallen, J. (2006). Multicellular rosette formation links planar cell polarity to tissue morphogenesis. *Dev. Cell* **11**, 459-470.
Brown, K., Baonza, A. and Freeman, M. (2006). Epithelial cell adhesion in the developing Drosophila retina is regulated by Atonal and the EGF receptor pathway. *Dev. Biol.* **300**, 710-721.
Cabernard, C. and Affolter, M. (2005). Distinct roles for two receptor tyrosine kinases in epithelial branching morphogenesis in Drosophila. *Dev. Cell* **9**, 831-842.
Ciruna, B. and Rossant, J. (2001). FGF signaling regulates mesoderm cell fate specification and morphogenetic movement at the primitive streak. *Dev. Cell* **1**, 37-49.
David, N. B., Sapede, D., Saint-Etienne, L., Thisse, C., Thisse, B., Dambly-Chaudiere, C., Rosa, F. M. and Ghysen, A. (2002). Molecular basis of cell migration in the fish lateral line: role of the chemokine receptor CXCR4 and of its ligand, SDF1. *Proc. Natl. Acad. Sci. USA* **99**, 16297-16302.
Dubrulle, J. and Pourquie, O. (2004). fgf8 mRNA decay establishes a gradient that couples axial elongation to patterning in the vertebrate embryo. *Nature* **427**, 419-422.
Dubrulle, J., McGrew, M. J. and Pourquie, O. (2001). FGF signaling controls somite boundary position and regulates segmentation clock control of spatiotemporal Hox gene activation. *Cell* **106**, 219-232.
Friedl, P., Hegerfeldt, Y. and Tusch, M. (2004). Collective cell migration in morphogenesis and cancer. *Int. J. Dev. Biol.* **48**, 441-449.
Geling, A., Steiner, H., Willem, M., Bally-Cuif, L. and Haass, C. (2002). A gamma-secretase inhibitor blocks Notch signaling in vivo and causes a severe neurogenic phenotype in zebrafish. *EMBO Rep.* **3**, 688-694.
Ghabrial, A. S. and Krasnow, M. A. (2006). Social interactions among epithelial cells during tracheal branching morphogenesis. *Nature* **441**, 746-749.
Ghysen, A. and Dambly-Chaudiere, C. (2007). The lateral line microcosmos. *Genes Dev.* **21**, 2118-2130.
Gryzik, T. and Muller, H. A. (2004). FGF8-like1 and FGF8-like2 encode putative ligands of the FGF receptor Htl and are required for mesoderm migration in the Drosophila gastrula. *Curr. Biol.* **14**, 659-667.
Haas, P. and Gilmour, D. (2006). Chemokine signaling mediates self-organizing tissue migration in the zebrafish lateral line. *Dev. Cell* **10**, 673-680.
Halloran, M. C., Sato-Maeda, M., Warren, J. T., Su, F., Lele, Z., Krone, P. H., Kuwada, J. Y. and Shoji, W. (2000). Laser-induced gene expression in specific cells of transgenic zebrafish. *Development* **127**, 1953-1960.
Henrique, D., Tyler, D., Kintner, C., Heath, J. K., Lewis, J. H., Ish-Horowicz, D. and Storey, K. G. (1997). cash4, a novel achaete-scute homolog induced by Hensen's node during generation of the posterior nervous system. *Genes Dev.* **11**, 603-615.
Herzog, W., Sonntag, C., von der Hardt, S., Roehl, H. H., Varga, Z. M. and Hammerschmidt, M. (2004). Fgf3 signaling from the ventral diencephalon is required for early specification and subsequent survival of the zebrafish adenohypophysis. *Development* **131**, 3681-3692.
Itoh, M. and Chitnis, A. (2001). Expression of proneural and neurogenic genes in the zebrafish lateral line primordium correlates with selection of hair cell fate in neuromasts. *Mech. Dev.* **102**, 263-266.
Jacinto, A. and Martin, P. (2001). Morphogenesis: unravelling the cell biology of hole closure. *Curr. Biol.* **11**, R705-R707.
Kimmel, C. B., Ballard, W. W., Kimmel, S. R., Ullmann, B. and Schilling, T. F. (1995). Stages of embryonic development of the zebrafish. *Dev. Dyn.* **203**, 253-310.
Kwan, K. M., Fujimoto, E., Grabher, C., Mangum, B. D., Hardy, M. E., Campbell, D. S., Parant, J. M., Yost, H. J., Kanki, J. P. and Chien, C. B. (2007). The Tol2kit: a multisite gateway-based construction kit for Tol2 transposon transgenesis constructs. *Dev. Dyn.* **236**, 3088-3099.
Lecaudey, V. and Gilmour, D. (2006). Organizing moving groups during morphogenesis. *Curr. Opin. Cell Biol.* **18**, 102-107.
Lee, Y., Grill, S., Sanchez, A., Murphy-Ryan, M. and Poss, K. D. (2005). Fgf signaling instructs position-dependent growth rate during zebrafish fin regeneration. *Development* **132**, 5173-5183.
Li, Q., Shirabe, K. and Kuwada, J. Y. (2004). Chemokine signaling regulates sensory cell migration in zebrafish. *Dev. Biol.* **269**, 123-136.
Martin, P. and Parkhurst, S. M. (2004). Parallels between tissue repair and embryo morphogenesis. *Development* **131**, 3021-3034.
Martin-Blanco, E. and Knust, E. (2001). Epithelial morphogenesis: filopodia at work. *Curr. Biol.* **11**, R28-R31.
Maves, L., Jackman, W. and Kimmel, C. B. (2002). FGF3 and FGF8 mediate a rhombomere 4 signaling activity in the zebrafish hindbrain. *Development* **129**, 3825-3837.
Millimaki, B. B., Sweet, E. M., Dhason, M. S. and Riley, B. B. (2007). Zebrafish atoh1 genes: classic proneural activity in the inner ear and regulation by Fgf and Notch. *Development* **134**, 295-305.
Munchberg, S. R., Ober, E. A. and Steinbeisser, H. (1999). Expression of the Ets transcription factors erm and pea3 in early zebrafish development. *Mech. Dev.* **88**, 233-236.
Nechiporuk, A., Linbo, T., Poss, K. D. and Raible, D. W. (2007). Specification of epibranchial placodes in zebrafish. *Development* **134**, 611-623.
Ng, J. K., Kawakami, Y., Buscher, D., Raya, A., Itoh, T., Koth, C. M., Rodriguez Esteban, C., Rodriguez-Leon, J., Garrity, D. M., Fishman, M. C. et al. (2002). The limb identity gene Tbx5 promotes limb initiation by interacting with Wnt2b and Fgf10. *Development* **129**, 5161-5170.

Norton, W. H., Ledin, J., Grandel, H. and Neumann, C. J. (2005). HSPG synthesis by zebrafish Ext2 and Extl3 is required for Fgf10 signalling during limb development. *Development* **132**, 4963-4973.
Pastor-Pareja, J. C., Grawe, F., Martin-Blanco, E. and Garcia-Bellido, A. (2004). Invasive cell behavior during Drosophila imaginal disc eversion is mediated by the JNK signaling cascade. *Dev. Cell* **7**, 387-399.
Pouthas, F., Girard, P., Lecaudey, V., Ly, T. B., Gilmour, D., Boulin, C., Pepperkok, R. and Reynaud, E. G. (2008). In migrating cells, the Golgi complex and the position of the centrosome depend on geometrical constraints of the substratum. *J. Cell Sci.* **121**, 2406-2414.
Ribeiro, C., Ebner, A. and Affolter, M. (2002). In vivo imaging reveals different cellular functions for FGF and Dpp signaling in tracheal branching morphogenesis. *Dev. Cell* **2**, 677-683.
Roehl, H. and Nusslein-Volhard, C. (2001). Zebrafish pea3 and erm are general targets of FGF8 signaling. *Curr. Biol.* **11**, 503-507.
Sarrazin, A., Villablanca, E., Nuñez, V., Sandoval, P., Ghysen, A. and Allende, M. (2006). Proneural gene requirement for hair cell differentiation in the zebrafish lateral line. *Dev. Biol.* **295**, 534-545.
Sutherland, D., Samakovlis, C. and Krasnow, M. A. (1996). branchless encodes a Drosophila FGF homolog that controls tracheal cell migration and the pattern of branching. *Cell* **87**, 1091-1101.
Thisse, B. and Thisse, C. (2005). Functions and regulations of fibroblast growth factor signaling during embryonic development. *Dev. Biol*. **287**, 390-402.
Wagstaff, L. J., Bellett, G., Mogensen, M. M. and Münsterberg, A. (2008). Multicellular rosette formation during cell ingression in the avian primitive streak. *Dev. Dyn*. **237**, 91-96.
Westerfield, M. (1995). *The Zebrafish Book. A Guide for the Laboratory Use of Zebrafish (Danio rerio)*. Eugene, OR: University of Oregon Press.
Xia, Y. and Karin, M. (2004). The control of cell motility and epithelial morphogenesis by Jun kinases. *Trends Cell Biol.* **14**, 94-101.
Yang, X., Dormann, D., Munsterberg, A. E. and Weijer, C. J. (2002). Cell movement patterns during gastrulation in the chick are controlled by positive and negative chemotaxis mediated by FGF4 and FGF8. *Dev. Cell* **3**, 425-437.
Zallen, J. A. and Blankenship, J. T. (2008). Multicellular dynamics during epithelial elongation. *Semin. Cell Dev. Biol.* **19**, 263-270.